Nat. Hazards Earth Syst. Sci. Discuss., 3, 5599–5632, 2015
www.nat-hazards-earth-syst-sci-discuss.net/3/5599/2015/
doi:10.5194/nhessd-3-5599-2015

Natural Hazards and Earth System Sciences Discussions
Open Access

A Quaternary Fault Database for Central Asia

S. Mohadjer[1], T. A. Ehlers[1], R. Bendick[2], K. Stübner[1], and T. Strube[1]

[1]Department of Geosciences, University of Tübingen, Wilhelmstrasse 56, 72074 Tübingen, Germany
[2]Department of Geosciences, University of Montana, 32 Campus Drive, Missoula, MT 59812, USA

Received: 27 July 2015 – Accepted: 25 August 2015 – Published: 23 September 2015

Correspondence to: S. Mohadjer (solmaz.mohadjer@gmail.com)

Published by Copernicus Publications on behalf of the European Geosciences Union.

Abstract

Earthquakes represent the highest risk in terms of potential loss of lives and economic damage for Central Asian countries. Knowledge of fault location and behavior is essential in calculating and mapping seismic hazard. Previous efforts in compiling fault information for Central Asia have generated a large amount of data that are published in limited-access journals with no digital maps publicly available, or are limited in their description of important fault parameters such as slip rates. This study builds on previous work by improving access to fault information through a web-based interactive map and an online database with search capabilities that allow users to organize data by different fields. The data presented in this compilation include fault location, its geographic, seismic and structural characteristics, short descriptions, narrative comments and references to peer-reviewed publications. The interactive map displays 1196 fault segments and 34 000 earthquake locations on a shaded-relief map. The online database contains attributes for 122 faults mentioned in the literature, with Quaternary and geodetic slip rates reported for 38 and 26 faults respectively, and earthquake history reported for 39 faults. This work has implications for seismic hazard studies in Central Asia as it summarizes important fault parameters, and can reduce earthquake risk by enhancing public access to information. It also allows scientists and hazard assessment teams to identify structures and regions where data gaps exist and future investigations are needed.

1 Introduction

The ongoing collision of the Indian subcontinent with Asia results in active deformation and seismicity in the Indo-Asian collision zone (Fig. 1). Continental collision initiated in the early Cenozoic (ca. 55 Ma) and is marked by large spatial and temporal variations in deformation across the Himalaya and surrounding areas (e.g., Hodges, 2000; Avouac, 2007; Thiede and Ehlers, 2013). India-Eurasia collision has created a complex zone

NHESSD

3, 5599–5632, 2015

A Quaternary Fault Database for Central Asia

S. Mohadjer et al.

of deformation that is characterized by an intricate network of faults, some of which have historically caused devastating earthquakes and continue to pose threats to the population at risk. Seven of the 28 deadliest earthquakes reported for 1990–2014 (USGS, 2014) are located in this zone with magnitudes ranging from 6.1 to 7.9 (Fig. 1). According to the United States Geological Survey, these events caused ~ 195 796 fatalities in total, corresponding to 23 % of total death toll reported for all deadly earthquakes in the world for the above period. Earthquakes in this region do not have to be particularly large to cause heavy damage. Only one of the 28 largest earthquakes reported for the above period is located within the India-Eurasia collision zone (i.e., the 2008 *M*7.9 Sichuan earthquake). Smaller events of magnitudes 6.1 and 6.6 that occurred in the Hindu Kush region in 2002 and 1998 respectively, caused over 5000 fatalities, left hundreds injured and several thousands homeless. To understand earthquakes and to address earthquake hazards, it is crucial to locate and characterize active faults accurately. In particular, fault location, earthquake history and cycle, as well as slip rate, are important input parameters that are used in calculations of earthquake hazards and probabilities. This information can serve as the basis for developing earthquake forecasts (Trifonov and Kozhurin, 2010; Wills et al., 2008; Plesch et al., 2007; Ruleman et al., 2007; Tapponnier et al., 2001).

Previous studies in Central Asia have produced a large amount of data that enhance our understanding of regional- and continental-scale tectonics as well as seismic hazards in the region. Geodetic measurements using the Global Positioning System (e.g., Bendick et al., 2015, 2007; Ischuk et al., 2013; Mohadjer et al., 2010; Zubovich et al., 2010; Reigber et al., 2001; Abdrakhmatov et al., 1996) and regional seismic investigations and catalogs (e.g., Schneider et al., 2013; Sippl et al., 2013; Mechie et al., 2012; Haberland et al., 2011; Mellors et al., 1995) continue to provide a more detailed pattern and rates of deformation associated with individual faults and other major structures. High resolution imagery allows for more accurate mapping of previously recognized faults and their geomorphic expressions (e.g., Chevalier et al., 2012; Robinson, 2009; Taylor and Yin, 2009; Strecker et al., 2003), and a significant

NHESSD
3, 5599–5632, 2015

number of previously unknown, but potentially active structures have been detected and interpreted based on satellite images and digital topographic data (e.g., Ruleman et al., 2007). Despite being limited in their coverage, recent paleoseismologic studies (e.g., Schiffman et al., 2013; Korjenkov et al., 2012; Ran et al., 2010; He et al., 2007; Kumar et al., 2006; Washburn et al., 2003) provide improved constraints on the magnitude and recurrence time of past earthquakes for some faults. The paleoseismic history of many faults, however, remains poorly understood. Previous investigations have often been limited to the Himalayan main frontal thrusts (Kumar et al., 2001 and 2006; Lavé et al., 2005) and other major structures such as the Kunlun and Altyn Tagh faults (He et al., 2007; Washburn et al., 2001 and 2003, respectively), or were only conducted in the aftermath of large events such as the 2005 Kashmir and the 2008 Sichuan earthquakes (Kaneda et al., 2008 and Ran et al., 2010, respectively). A more complete paleoseismic record can enhance our understanding of fault behavior and earthquake hazard in the region. All data from previous work provide baseline observation for understanding patterns and rates of active faulting in Central Asia.

Despite considerable advancements provided by previous work, there are several shortcomings that impede information sharing and adequate assessment of fault activity and hazards in the region. Previous investigations have generated data that are documented in a wide range of formats (e.g., digital, texts, maps, and images) that are often published in non-open access journals. This can make access, usage, and dissemination of fault data a time consuming and resource intensive task, particularly for non-academic users and the general public. Despite initiatives that aim to provide a centralized platform for storage, maintenance, and the display of fault data specific to other regions of the world such as the online Quaternary Fault and Fold Database of the United States Geological Survey (http://earthquake.usgs.gov/hazards/qfaults/), few attempts have been made for Central Asian faults (e.g., Ioffe and Kozhurin, 1996; Ioffe et al., 1993; Trifonov, 2000). The HimaTibetMap of Taylor and Yin (2009) is currently the only publicly available digital database of active structures located in Central Asia. Users can download and view fault location data on a semi-interactive map. The fault data, however, are unsearchable and limited to a few parameters only. The Global Earthquake Model Global Active Faults Database (http://www.globalquakemodel.org/) is currently being tested with no fault data from Central Asia. Therefore, there is a clear need for an open-access database with fault information that focuses on Central Asia.

Our work compliments previous efforts by providing an open-access and searchable database that includes an interactive map that is linked to an online database. Database users can generate simple and complex queries to access and view not only fault locations, but also important fault parameters such as slip rates and earthquake history. All data stored and displayed in the database are the product of work in progress and subject to change based on community's feedback and future refinement as more studies become available. An objective of this work is to make fault information available to not only the science community, but also to the general public and encourage local and international organizations to consider fault location and parameters in their project analysis.

2 Datasets

The Central Asia Fault Database (CAFD) contains three different datasets including fault locations, fault attributes, and seismicity (Table 1). Fault locations show the position of 1196 active fault segments that have been mapped or show surface expressions. The term "active" is used to refer to faults that have moved within the Quaternary Period ($\lesssim$2.6 Ma). Fault attributes (Table 2) for 122 faults are divided into six categories (i.e., identifiers, geographic characteristics, seismic characteristics, structural characteristics, description and references). Each category contains fields that show relevant fault information. The database fields range from fault name, exposure and country to Quaternary and geodetic slip rates, earthquake history, geomorphic markers of activity, paleoseismic data, and fault length and sense of motion. Additionally, a brief description and a list of references are provided for each fault. Table 3 provides a more detailed description for each field. Seismicity data include location, magnitude, and depth of over 34 000 earthquakes that were recorded throughout the region using global (ANSS ComCat, 2014) and regional (Sippl et al., 2013) seismic networks. All datasets are based on our review of over 250 published manuscripts. The forthcoming sections provide a more detailed description of each dataset, and the criteria used for dataset selection and evaluation.

2.1 Fault locations

Detailed and accurate mapping of fault systems and subsidiary features are essential to understanding of fault characteristics and activity. Precise fault locations can also aid with identification of promising sites for paleoseismic and geomorphic investigations (Zachariasen and Prentice, 2008). Locations of the 1196 fault segments in the current version of CAFD are based on maps and figures that come from 84 published studies. These studies include both those that have broadly defined the location and behavior of active faults (e.g., northern extension of the Chaman fault in Afghanistan) and those that more accurately have mapped and described individual strands of fault systems (e.g., Karakoram fault strands). The latter was chosen for the database when available. The database contains 569 fault traces from the HimaTibetMap of Taylor and Yin (2009), which is an open-source digital database of active faults located in the Indo-Asian collision zone. The faults taken from the HimaTibetMap are based on field observations and interpretations of satellite images and digital topographic data (Styron et al., 2010; Taylor and Yin, 2009; Taylor et al., 2003) as well as other previously published work.

When digitized data are not available, individual fault traces were digitized from their original sources and at the original publication map scale using the ArcMap software. To digitize a fault, a map is first aligned to available datasets (e.g., country boundaries) and then georeferenced using more accurate data layers such as ASTER GDEM2 (30 m resolution digital topography). The fault traces are then digitized and linked to an attribute table in ArcMap. The attribute table contains information about each fault including its name, sense of movement (if known),

NHESSD
3, 5599–5632, 2015

references, and other important remarks such as variations in the fault name or location. Fault location accuracy depends on the scale of observation used in previous investigations. Since investigations were conducted at a variety of different scales and methods, some structures are located more precisely than others. For example, Ruleman et al. (2007) mapped features mostly from 90 m-resolution Landsat ETM (Enhanced Thematic Mapper) data at a maximum scale of about 1 : 50 000 (∼ 25 m raster resolution) while Schurr et al. (2014) relied on 1 : 200 000 maps (∼ 100 m raster resolution) for their interpretation of Cenozoic faults. To increase location accuracy, Schurr et al. (2014) also used satellite imagery and fieldwork. These examples demonstrate that uncertainties in the positions of each fault in this database are variable, and therefore, users are encouraged to consult the original source provided in the comments field within the database for a detailed understanding of the location uncertainties associated with each fault.

In general, the position accuracy for each fault is suitable for visualizing and plotting faults at a regional scale and most likely not suited for site-specific studies without consulting the original study provided in the references. When there are discrepancies in fault locations, we adjusted the position of previously mapped faults to coincide with surface features visible in ASTER GDEM2 data that are indicative of their trace. This is noted in the comment fields of the database. Faults with an undetermined level of activity (e.g., Herat fault in Afghanistan) are included in the database to avoid creating false impressions about seismic hazard and risk in some localities. Finally, faults not documented in this study exist and may be active, but are unfortunately not yet documented sufficiently for inclusion in this study.

2.2 Fault attributes

All fault parameters used in the database fields (Table 3) are documented from original sources. More specific information about each parameter is reported in the comments field within the database, especially where discrepancies exist. The most common database fields with comments include fault name, exposure level, geodetic

NHESSD
3, 5599–5632, 2015

and geologic slip rates, and sense of motion. The comments field for fault name explains different names used to refer to the same fault including variations in spelling (e.g., North Pamir Thrust is also referred to as Main Pamir Thrust, Main Alai Thrust, and Pamir Thrust System). Similarly, the fault exposure comments are used for faults with varying levels of surface exposure (e.g., Himalayan Main Frontal Thrust being concealed within the mapping area of Raiverman et al. (1993) but displaying morphology indicative of surface faulting near Chapri rao and west of the Tamuna River as shown in Wesnousky et al., 1999). Additional data for slip rates such as type, uncertainties and locations are included in the relevant comments fields. Where different types of fault movements are reported for the same structure (e.g., thrust with component of left-lateral shear reported for Oinak–Djar Fault) or when a fault's style of movement changes along its length (e.g., Konar fault showing a progressively greater component of thrust faulting northeastward), the comments field reflects this information. Comments fields can also include references used for an entry in a database field. Important fault attributes such as Quaternary and geodetic slip rates are discussed in more detail below.

2.3 Slip rates

Slip rate data are important parameters in determining seismic hazard as they can aid in estimating recurrence intervals for earthquakes. The CAFD documents both Quaternary and geodetic slip rates for faults. Quaternary slip rates are often used in seismic hazard models as these values are thought to better represent deformation rates appropriate for hazard models (Field et al., 2013). Where these rates are lacking or inaccurate, particularly in locations with no evidence for old or recent earthquakes, geodetic rates from GPS or InSAR are used to determine present-day deformation rates for faults. These rates include interseismic, coseismic, and post-seismic motions, yielding information that can help with identification of locked fault segments or faults with slow-slip motions. In the database, both slip rates are reported in millimeters per year, showing minimum and maximum reported values from published literature.

NHESSD
3, 5599–5632, 2015

Figure 2 shows the distribution of geodetic and Quaternary slip rates for faults included in the database. Geodetic slip rates are reported for 26 faults, with values ranging from < 5 to $< 30\,\mathrm{mm\,yr^{-1}}$, with most rates reported as maximums with values between 10 and $15\,\mathrm{mm\,yr^{-1}}$, and as minimums with values $< 5\,\mathrm{mm\,yr^{-1}}$ (Fig. 2a). Quaternary slip rates reported for 38 faults show values ranging from < 5 to $40\,\mathrm{mm\,yr^{-1}}$, with most rates reported as minimum with values $< 5\,\mathrm{mm\,yr^{-1}}$ (Fig. 2b). There are only 20 faults that have both Quaternary and geodetic slip rates. Corresponding uncertainties in fault slip rates as well as other supporting data such as site location, offset geomorphic feature, and dating method for offset features are reported from the original studies and are included in the comments fields of the database.

2.4 Seismicity

The earthquakes in the current version of CAFD include over 25 000 events from the Advance National Seismic System Comprehensive Catalog (ANSS ComCat). These events were recorded by over 150 seismic stations distributed globally over 80 countries as part of the Global Seismographic Network (Gee and Leith, 2011). The events cover a period from 1900 to 2014. The magnitude for each event is calculated using several different methods, depending upon the type of earthquake, the amount of energy released, and the policies of the authoritative seismic network. The position uncertainty of a hypocenter location of an event in the ANSS ComCat is defined by its epicenter and focal depth, and is estimated to be about 10 s of kilometers. Since the accuracy in determining the epicenter location, depth, and size of an earthquake is a function of the geometry and density of seismograph networks and available seismic data (Husen and Hardebeck, 2010), smaller sized events ($M < 5$) in the database must be treated with caution as they are unlikely to have been accurately located.

The ANSS global catalog is complemented by events from local networks and other temporary station deployments in the Pamir, Hindu Kush and South Tien Shan. The database displays over 9000 events from the local TIPAGE (TIen Shan PAmir GEodynamic Program) catalog. These events were detected by a network of

NHESSD
3, 5599–5632, 2015

40 seismic stations in southern Kyrgyzstan and eastern Tajikistan over a period of two years from August 2008 to June 2010. Sippl et al. (2013) used a probabilistic earthquake relocation method (Lomax et al., 2000) to measure absolute location errors. They estimated mean location uncertainties in longitudinal, latitudinal and vertical directions, calculated for bins in different depth layers. Their results show vertical errors being larger than horizontal errors for all events, with horizontal errors lower than 7.5 km and vertical errors lower than 15 km throughout the Pamir.

In the database, all earthquakes are sorted based on their size (i.e., below or above magnitude 5) and depth (i.e., below or above 70 km depth). Events below magnitude 5 are considered to have intensity values of I–V on the Modified Mercalli Intensity Scale used by the United States Geological Survey, indicating micro to light shaking effects. Events over magnitude 5 are given intensity values of VI–VIII or above indicating moderate to great shaking effects that are felt over large areas and causing damage to structures. Events between 0 and 70 km are considered to be shallow while those above 70 km are intermediate or deep events. The earthquake locations are indicated by circles, each representing an earthquake's epicenter. Figure 3 shows the distribution of earthquakes from both catalogs based on magnitude and depth. Most events in both catalogs have magnitudes below 5 (Fig. 3a). Events with magnitudes between 1 and 3 are captured by the TIPAGE regional network whereas events with magnitudes above 5 are captured mostly by the ANSS global catalog. By combining these datasets, the database provides a more complete overview of past event magnitudes. Most events in both catalogs show depths of 50 km below surface (Fig. 3b) with deeper events (> 250 km) represented by the ANSS global catalog only. In the east of Alai valley and within the Pamir thrust system, the 2008 Nura earthquake and its aftershock series (∼ 3000 events) are captured by the TIPAGE catalog, and are included in the database in different color (Fig. 5b) to allow users to differentiate them from background seismicity in the Alai valley.

NHESSD
3, 5599–5632, 2015

3 Database construction

The CAFD construction follows four steps (Fig. 4). First, previously published literature and databases related to Quaternary faulting in Central Asia were compiled and reviewed. Fault trace data were prepared in the ArcMap software, and used to populate tables created in a MySQL database using an open source, web-based application called phpMyAdmin (https://www.phpmyadmin.net/). The MySQL database is composed of data tables that can be queried. The fault location table was created to store geographic coordinates (i.e., latitude, longitude) of points that made up a fault trace. The fault attribute table was created to organize attribute information shown in Tables 2–3. To link the fault location table to the fault attribute table, a unique identification number was assigned to each fault and used in both tables. Using PHP scripting (http://www.php.net/), the fault location and attribute data were then extracted from these tables for display in an open source web-mapping application called OpenLayers (http://openlayers.org/). To display earthquake data, a table was created in the database to store location coordinates, depth, magnitude, and source values. These data were similarly extracted from the database for display in OpenLayers. The reference table was created and displayed similarly, containing fields such as fault identification number, citation appearance, and manuscript title. This table was used to generate an automated query in Google Scholar by clicking on a citation listed for a fault. All raw data in the CAFD are accessible for viewing and download via http://www.geo.uni-tuebingen.de/faults/ and the Supplement accompanying this article. Users who download the data are encouraged to regularly check for new entries or subscribe to the email list server for this database.

4 User interface

The CAFD online interface includes an interactive fault map and a search tool. The fault map displays the locations of active faults (Fig. 5a) and includes a user-controlled

NHESSD
3, 5599–5632, 2015

earthquake data layer (Fig. 5b) that organizes data by magnitude, depth and source. Clicking on a fault trace brings up an information page (Fig. 6) that is linked to the fault attribute and reference tables in the database, displaying relevant information organized by database fields (Table 3). The information page also contains a location map that highlights the fault location.

The search tool (Fig. 7) allows users to query the database using specific fields. Table 2 shows fields that are queryable. The queries can be simple (e.g., fault name or country location) or more complex (e.g., sorted by slip rate, sense of motion, earthquake history, etc.). A query can generate results (i.e., fault names shown in a list and on a map) that are linked to fault information and location pages described above.

5 Database completeness

The main objective of the CAFD is to provide a publicly accessible central source of information related to active faults in Central Asia and to set a framework for future data additions and research. Similar to the HimaTibetMap of Taylor and Yin (2009), the data in the CAFD are drawn from published manuscripts that are based on limited set of data, and require continual evaluation as newer data become available. For example, a large number of faults lack geodetic or Quaternary slip rates, and most faults contain no paleoseismic information.

Although the database has implications for seismic hazard studies in Central Asia, it is impractical to construct a hazard map based solely on the information provided here. The database contains active faults with surface traces, providing only a two-dimensional representation of faults and potentially leaving out active nonplanar faults and those that are concealed beneath the Earth's surface. The accuracy of fault position data for faults with surface traces also depends on mapping methods and scales of observations, which vary significantly between individual studies. Similarly, the accuracy of fault attributes can vary between individual studies. For example, fault slip rate measurements are based on estimates of displacements along faults and

NHESSD
3, 5599–5632, 2015

age measurements of offset landforms, both of which contain uncertainties that are obtained and reported differently across referenced studies. Database users, therefore, are encouraged to refer to comments fields in the database for more information about reported values, and to references cited for original work. These limitations combined with short seismological records and insufficient information about earthquake shaking intensities are a great challenge to mapping hazards in the region. A more complete hazard assessment process should consider long-term earthquake history of faults (available from paleoseismic data), GPS velocity data showing present-day strain accumulation across active structures, and more accurate mapping of active faults, especially those with no clear surface expression (e.g., blind faults).

5.1 Data gaps

At its current stage, the database guides future research by identifying areas where further investigations are needed. Figure 8 shows the locations of active faults as documented in the database, color-coded based on their sense of motion. Although the sense of motion for most active structures is well-characterized, slip rates for most remain unknown. Slip rates are reported for a total of 64 faults in the current version of the CAFD. This includes 26 geodetic and 38 Quaternary rates. Only 20 faults, however, have both types of slip rates. These faults are often > 1000 km long and bound major topographic features (e.g., the ∼ 1200 km-long Altyn-Tagh fault at the northern margin of the Tibetan Plateau, the > 1500 km-long Main Frontal thrust system along the Himalaya, and the ∼ 1000 km-long Chaman fault system that bounds the western edge of the Indian Plate). Some faults such as the Altyn Tagh, Kunlun and Karakoram have Quaternary slip rates that are constrained by several studies in different localities along the fault trace. Other fault zones such as those in northwest of Tibet and the Central Pamir, require further investigation. Quaternary slip rates in this region are often qualitative, associated with large uncertainty (e.g., the Darvaz Karakul fault) or disagree with GPS measurements (e.g., the Talas Ferghana and Karakorum faults).

NHESSD
3, 5599–5632, 2015

The northern and western margins of the Pamir have geodetic relative velocities of 13–15 and 10 mm yr^{-1} respectively. Quaternary slip rates for these areas are only available for the central segment of the Pamir thrust system. Therefore, where and how these motions are accommodated remains poorly understood. Unlike central Tibet where Quaternary and geodetic slip rates are known for several fault systems (e.g., Bue Co and Dong Co conjugate fault systems), the faults located in the interior of the Pamir lack Quaternary rates despite accommodating 5–10 mm yr^{-1} of east–west extension measured by GPS geodesy (Ischuk et al., 2013).

Further south, few geologic and geodetic constraints exist on slip rates for faults in Afghanistan and the Baluchistan province of Pakistan. The only available geodetic rates are for the Chaman fault system and its northern (e.g., Gardiz and Mokur faults) and southern (e.g., Ornach–Nal and Ghazaband faults) extensions. Despite constraints placed by deformation models on the present-day kinematics of regions south and west of the western Himalayan Syntaxis (e.g., the Sulaiman Lobe and Range), it remains unclear exactly how and where this deformation is accommodated. The database highlights regions and fault systems that have well-constrained slip rate data and those that lack such data, and hence, can guide future research by identifying where data gaps exist.

6 Database maintenance

All domain and web hosting services are provided and maintained by the University of Tübingen. The content update is a collaborative process which includes content identification, content review and database update. Content identification is done by a group of experts who are selected and contacted semiannually for published research results. A larger number of potential experts and users are also contacted using selected list servers. Users can submit new content directly via the website email (cafd@ifg.uni-tuebingen.de) or by completing the feedback form on the website. Once

NHESSD
3, 5599–5632, 2015
A Quaternary Fault Database for Central Asia
S. Mohadjer et al.

content is submitted, it is checked for accuracy and consistency by the CAFD review team before being posted on the website.

7 Conclusions

The Central Asia Fault Database contains 1196 fault segments that can be viewed, searched, and downloaded for plotting in ArcGIS and other programs. Fault parameters and descriptions for over 122 active faults are extracted and documented in the database and can be searched and viewed by users. Over 34 000 earthquakes from global and local catalogs are included in data layers to explore the relationship between seismicity and active faulting. This database is the first publicly available digital repository for active faults of Central Asia and the surrounding region with search capabilities that allow users sort and view critical fault information on a variety of fields (e.g., geographic, seismic, geomorphic, structural). This information is critical for current and future analysis of earthquake hazard studies in the region. The database is designed to fulfill the needs of a wide range of users ranging from the science community to the general public and non-academic users. The database will be continuously updated as new information becomes available and as users identify data that have been overlooked using a web-based discussion forum or contacting the authors directly.

The Supplement related to this article is available online at doi:10.5194/nhessd-3-5599-2015-supplement.

Author contributions. S. Mohadjer assembled input data from literature, and designed and populated the database with the help of T. Strube; T. Strube wrote the php and java scripts required for displaying data and website development; T. A. Ehlers and R. Bendick contributed to project planning and database design. K. Stübner provided input on database construction and data display. All authors contributed to manuscript preparation.

NHESSD
3, 5599–5632, 2015

Acknowledgements. We thank Steve Thompson, Ray Weldon, Mike Taylor, Richard Styron, Cal Ruleman, Bernd Schurr, and Richard Gloaguen for generously sharing their data. We also thank Peter Molnar, Roger Bilham, and Kathleen Haller for their helpful discussions. Saeid Mohadjer, Faheem Merchant, Stéphane Henroid, Cassidy Jay, and Najibullah Kakar provided thoughtful feedback on website design, usability and content. Roland Schraven assisted with preparing earthquake and topography data used in this manuscript. In its early stage, this project benefited immensely from fruitful discussions with Michael Märker, Jason Barnes, and Lothar Ratschbacher. This project was supported by the CAME project bundle TIPTIMON of the German Federal Ministry of Education and Research grant BMBF 03G0809 (to T. A. Ehlers) and the German Science Foundation grant STU 525/1–1 (to K. Stübner).

References

Abdrakhmatov, K. Y., Aldazhanov, S. A., Hager, B. H., Hamburger, M. W., Herring, T. A., Kalabaev, K. B., Makarov, V. I., Molnar, P., Panasyuk, S. V., Prilepin, M. T., Reilinger, R. E., Sadybakasov, I. S., Souter, B. J., Trapeznikov, Y. A., Tsurkov, V. Y., and Zubovich, A. V.: Relatively recent construction of the Tien Shan inferred from GPS, Nature, 384, 450–453, 1996.

Advance National Seismic System Comprehensive Catalog (ANSS ComCat): available at: http://earthquake.usgs.gov/earthquakes/search/, last access: December 2014.

Avouac, J. P.: Dynamic processes in extensional and compressional settings – mountain building from earthquakes to geological deformation, in: Treatise on Geophysics, edited by: Schubert, G., Elsevier, Amsterdam, 377–439, 2007.

Bendick, R., Bilham, R., Khan, M. A., and Khan, S. F.: Slip on active wedge thrust from geodetic observations of the 8 October 2005 Kashmir earthquake, Geology, 35, 267–270, 2007.

Bendick, R., Khan, S. F., Bürgmann, R., Jouanne, F., Banerjee, P., Khan, M. A., and Bilham, R.: Postseismic relaxation in Kashmir and lateral variations in crustal architecture and materials, Geophys. Res. Lett., 42, 4375–4383, 2015.

Chevalier, M. L., Tapponnier, P., Van der Woerd, J., Ryerson, F. J.,Finkel, R. C., and Li, H.: Spatially constant slip rate along the southern segment of the Karakorum fault since 200 ka, Tectonophysics, 530–531, 152–179, 2012.

NHESSD

3, 5599–5632, 2015

A Quaternary Fault Database for Central Asia

S. Mohadjer et al.

Field, E. H., Biasi, G. P., Bird, P., Dawson, T. E., Felzer, K. R., Jackson, D. D., Johnson, K. M., Jordan, T. H., Madden, C., Michael, A. J., Milner, K. R., Page, M. T., Parsons, T., Powers, P. M., Shaw, B. E., Thatcher, W. R., Weldon II, R. J., and Zeng, Y.: Uniform California earthquake rupture forecast, version 3 (UCERF3) – The time-independent model: U.S. Geological Survey Open-File Report 2013–1165, 97 pp., California Geological Survey Special Report 228, and Southern California Earthquake Center Publication 1792, available at: http://pubs.usgs.gov/of/2013/1165/, last access: June 2015, 2013.

Gee, L. S. and Leith, W. S.: The Global Seismographic Network: United States Geological Survey, Fact Sheet 2011–3021, available at: http://pubs.usgs.gov/fs/2011/3021/, last access: May 2015, 2011.

Haberland, C., Abdybachaev, U., Schurr, B., Wetzel, H.-U., Roessner, S., Sarnagoev, A., Orunbaev, S., and Janssen, C.: Landslides in southern Kyrgyzstan: understanding tectonic controls, Eos T. Am. Geophys. Un., 92, 169–170, 2011.

He, W., Xiong, Z., Yuan, D. Y., Ge, W. P., and Liu, X. W.: Paleo-earthquake study on the Maqu fault of East Kunlun Active Fault, Earthquake Research China, 22, 126–133, 2007 (in Chinese with English abstract).

Hodges, K.: Tectonics of the Himalaya and southern Tibet from two perspectives, Geol. Soc. Am. Bull., 112, 324–350, 2000.

Husen, S. and Hardebeck, J. L.: Earthquake location accuracy, Community Online Resources for Statistical Seismicity Analysis (CORSSA), version 1, doi:10.5078/corssa-55815573, available at: http://www.corssa.org/articles/themeiv/husen_hardebeck/husen_hardebeck.pdf, last access: June 2015, 2010.

Ioffe, A., Govorova, N., Volchkova, G., and Trifonov, R.: Database of active faults for the USSR area, Geoinformatics, 4, 289–290, 1993.

Ioffe, A. I. and Kozhurin, A. I.: Database of active faults of Eurasia, Journal of Earthquake Prediction Research, 5, 431–435, 1996.

Ischuk, A., Bendick, R., Rybin, R., Molnar, P., Khan, S. F., Kuzikov, S., Mohadjer, S., Saydullaev, U., Ilyasova, Z., Schelochkov, G., and Zubovich, A. V.: Kinematics of the Pamir and Hindu Kush regions from GPS geodesy, J. Geophys. Res.-Sol. Ea., 118, 1–9, 2013.

Kaneda, H., Nakata, T., Tsutsumi, H., Kondo, H., Sugito, N., Awata, Y., Akhtar, S. S., Majid, A., Khattak, W., Awan, A. A., Yeats, R. S., Hussain, A., Ashraf, M., Wesnousky, S. G., and Kausar, A. B.: Surface rupture of the 2005 Kashmir, Pakistan, earthquake and its active tectonic implications, B. Seismol. Soc. Am., 98, 521–557, doi:10.1785/0120070073, 2008.

NHESSD
3, 5599–5632, 2015

A Quaternary Fault Database for Central Asia

S. Mohadjer et al.

Korjenkov, A. M., Rust, D., Tibaldi, A., and Abdieva, S. V.: Parameters of the Strong Paleoearthquakes Along the Talas-Fergana Fault, the Kyrgyz Tien Shan, in: Earthquake Research and Analysis – Seismology, Seismotectonic and Earthquake Geology, edited by: D'Amico, S., InTech, Croatia, 2012.

Kumar, S., Wesnousky, S. G., Rockwell, T. K., Ragona, D., Thakur, V. C., and Seitz, G. G.: Earthquake recurrence and rupture dynamics of Himalayan Frontal Thrust, India, Science, 294, 2328–2332, 2001.

Kumar, S., Wesnousky, S. G., Rockwell, T. K., Briggs, R. W., Thakur, V. C., and Jayangondaperumal, R.: Paleoseismic evidence of great surface rupture earthquakes along the Indian Himalaya, J. Geophys. Res.-Sol. Ea., 111, B03304, doi:10.1029/2004JB003309, 2006.

Lavé, J., Yule, D., Sapkota, S., Basant, K., Madden, C., Attal, M., and Pandey, R.: Evidence for a Great Medieval Earthquake (~ 1100 A. D.) in the Central Himalayas, Nepal, Science, 307, 1302–1305, doi:10.1126/science.1104804, 2005.

Lomax, A., Virieux, J., Volant, P., and Berge, C.: Probabilistic earthquake location in 3D and layered models: Introduction of a Metropolis-Gibbs method and comparison with linear locations, in: Advances in Seismic Event Location, edited by: Thurber, C. and Rabinowitz, N., Kluwer, Amsterdam, 101–134, 2000.

Mechie, J., Yuan, X., Schurr, B., Schneider, F., Sippl, C., Ratschbacher, L., Minaev, V., Gadoev, M., Oimahmadov, I., Abdybachaev, U., Moldobekov, B., Orunbaev, S., and Negmatullaev, S.: Crustal and uppermost mantle velocity structure along a profile across the Pamir and southern Tien Shan as derived from project TIPAGE wide-angle seismic data, Geophys. J. Int., 188, 385–407, 2012.

Mellors, R. J., Pavlis, G. L., Hamburger, M. W., Al-shukri, H. J., and Lukk, A. A.: Evidence for a high velocity slab associated with the Hindu Kush seismic zone, J. Geophys. Res.-Sol. Ea., 100, 4067–4078, 1995.

Mohadjer, S., Bendick, R., Ischuk, A., Kuzikov, S., Kostuk, A., Saydullaev, U., Lodi, S., Kakar, D. M., Wasy, A., Khan, M. A., Molnar, P., Bilham, R., and Zubovich, A. V.: Partitioning of India-Eurasia convergence in the Pamir-Hindu Kush from GPS measurements, Geophys. Res. Lett., 37, L04305, doi:10.1029/2009GL041737, 2010.

Plesch, A., Shaw, J. H., Benson, C., Bryant, W. A., Carena, S., Cooke, M., Dolan, J., Fuis, G., Gath, E., Grant, L., Hauksson, E., Jordan, T., Kamerling, M., Legg, M., Lindvall, S., Magistrale, H., Nicholson, C., Niemi, N., Oskin, M., Perry, S., Planansky, G., Rockwell, T.,

Shearer, P., Sorlien, C., Süss, M. P., Suppe, J., Treiman, J., and Yeats, R.: Community Fault Model (CFM) for Southern California, B. Seismol. Soc. Am., 97, 1793–1802, 2007.
Raiverman, V., Srivastava, A. K., and Prasad, D. N.: On the Foothill Thrust of northwestern Himalaya, Journal of Himalayan Geology, 4, 237–256, 1993.
Ran, Y., Chen, L., Chen, J., Wang, H., Chen, G, Yin, J., Shi, X., Li, C., and Xu, X.: Paleoseismic evidence and repeat time of large earthquakes at three sites along the Longmenshan fault zone, Tectonophysics, 491, 141–153, 2010.
Reigber, C., Michel, G. W., Galas, R., Angermann, D., Klotz, J., Chen, J. Y., Papschev, A., Arslanov, R., Tzurkov, V. E., and Ishanov, M. C.: New space geodetic constraints on the distribution of deformation in Central Asia, Earth Planet. Sc. Lett., 191, 157–165, 2001.
Robinson, A. C.: Geologic offsets across the northern Karakorum fault: implications for its role and terrane correlations in the western Himalayan-Tibetan orogen, Earth Planet. Sc. Lett., 279, 123–130, 2009.
Ruleman, C. A., Crone, A. J., Machette, M. N., Haller, K. M., and Rukstales, K. S.: Map and Database of Probable and Possible Quaternary Faults in Afghanistan, United States Geological Survey Open-File Report, 2007-1103, available at: http://pubs.usgs.gov/of/2007/1103/, last access: July 2015, 2007.
Schiffman, C., Bali, B. S., Szeliga, W., and Bilham, R.: Seismic slip deficit in the Kashmir Himalaya from GPS observations, Geophys. Res. Lett., 40, 5642–5645, 2013.
Schneider, F. M., Yuan, X., Schurr, B., Mechie, J., Sippl, C., Haberland, C., Minaev, V., Oimahmadov, I., Gadoev, M., Radjabov, N., Abdybachaev, U., Orunbaev, S., and Negmatullaev, S.: Seismic imaging of subducting continental lower crust beneath the Pamir, Earth Planet. Sc. Lett., 375, 101–112, 2013.
Schurr, B., Ratschbacher, L., Sippl, C., Gloaguen, R., Yuan, X., and Mechie, J.: Seismotectonics of the Pamir, Tectonics, 33, 1501–1518, 2014.
Sippl, C., Schurr, B., Yuan, X., Mechie, J., Schneider, F. M., Gadoev, M., Orunbaev, S., Oimahmadov, I., Haberland, C., Abdybachaev, U., Minaev, V., Negmatullaev, S., and Radjabov, N.: Geometry of the Pamir-Hindu Kush intermediate-depth earthquake zone from local seismic data, J. Geophys. Res.-Sol. Ea., 118, 1438–1457, 2013.
Strecker, M. R., Hilley, G. E., Arrowsmith, J. R., and Coutand, I.: Differential structural and geomorphic mountain-front evolution in an active continental collision zone: the northwest Pamir, southern Kyrgyzstan, Geol. Soc. Am. Bull., 115, 166–181, 2003.

NHESSD
3, 5599–5632, 2015

Styron, R., Taylor, M., and Okoronkwo, K.: Database of active structures from the Indo-Asian Collision, Eos T. Am. Geophys. Un., 91, 181–182, 2010.
Tapponnier, P., Ryersonb, F. J., Van der Woerda, J., Mériauxa, A. S., and Lasserrea, C.: Long-term slip rates and characteristic slip: keys to active fault behavior and earthquake hazard, Earth Planet. Sc. Lett., 333, 483–494, 2001.
Taylor, M. and Yin, A.: Active structures of the Himalayan-Tibetan orogen and their relationships to earthquake distribution, contemporary strain field, and Cenozoic volcanism, Geosphere, 5, 199–214, 2009.
Taylor, M., Yin, A., Ryerson, F., Kapp, P., and Ding, L.: Conjugate strike slip fault accommodates coeval north–south shortening and east–west extension along the Bangong-Nujiang suture zone in central Tibet, Tectonics, 22, 1044, doi:10.1029/2002TC001361, 2003.
Thiede, R. C. and Ehlers, T. A.: Large spatial and temporal variations in Himalayan denudation, Earth Planet. Sc. Lett., 371, 278–293, 2013.
Trifonov, V. G.: Using active faults for estimating seismic hazard, Journal of Earthquake Prediction Research, 8, 170–182, 2000.
Trifonov, V. G. and Kozhurin, A. I.: Study of active faults: theoretical and applied implications, Geotectonics, 44, 510–528, 2010.
United Stated Geological Survey (USGS): Largest and Deadliest Earthquakes by Year: 1990–2014, available at: http://earthquake.usgs.gov/earthquakes/eqarchives/year/byyear.php (last access: 24 July 2015), 2014.
Washburn, Z., Arrowsmith, J. R., Forman, S., Cowgill, E., Wang, X. F., Zhang, Y., and Zhengle, C.: Late Holocene earthquake history of the Central Altyn Tagh Fault, China, Geology, 29, 1051–1054, 2001.
Washburn, Z., Arrowsmith, J. R., Dupont-Nivet, G., Feng, W. X., Qiao, Z. Y., and Zhengle, C.: Paleoseismology of the Xorxol Segment of the Central Altyn Tagh Fault, Xinjiang, China, Ann. Geophys.-Italy, 46, 1015–1034, 2003.
Wesnousky, S. G., Kumar, S., Mohindra, R., and Thakur, V. C.: Uplift and convergence along the Himalayan Frontal Thrust of India, Tectonics, 18, 967–976, 1999.
Wills, C. J., Weldon II, R. J., and Bryant, W. A.: California fault parameters for the National Seismic Hazard Maps and Working Group on California Earthquake Probabilities, Appendix A in The Uniform California Earthquake Rupture Forecast, version 2 (UCERF 2): U. S. Geological Survey Open-File Report 2007–1437A, and California Geological Survey Special

NHESSD
3, 5599–5632, 2015

Report 203A, 48, available at: http://pubs.usgs.gov/of/2007/1437/a/, last access: June 2015, 2008.
Zachariasen, J. and Prentice, C. S.: Detailed Mapping of the Northern San Andreas Fault Using LiDAR Imagery, United Stated Geological Survey Final Technical Report 05HQGR0069, 1–47, available at: http://earthquake.usgs.gov/research/external/reports/05HQGR0069.pdf, last access: July 2015, 2008.
Zubovich, A. V., Wang, X., Scherba, Y. G., Schelochkov, G. G., Reilinger, R., Reigber, C., Mosienko, O. I., Molnar, P., Michajljow, W., Makarov, V. I., Li, J., Kuzikov, S. I., Herring, T. A., Hamburger, M. W., Hager, B. H., Dang, Y., Bragin, V. D., and Beisenbaev, R. T.: GPS velocity field for the Tien Shan and surround region, Tectonics, 29, TC6014, doi:10.1029/2010TC002772, 2010.

NHESSD
3, 5599–5632, 2015

Table 1. Overview of the data sets used in the CAFD.

Data	# of entries	Source	Remarks
Fault locations	1196 fault segments	Published literature	Faults with Quaternary deformation (<∼ 2.6 Ma)
Fault attributes	122 faults		
Earthquakes	25 000 earthquakes 9000 earthquakes	TIPAGE (Sippl et al., 2013) ANSS ComCat (ANSS, 2014)	Aug 2008–Jun 2010 1900–2014

NHESSD
3, 5599–5632, 2015

Table 2. Structure of the CAFD and queryable search fields.

		Database fields	Queryable
Fault system	Identifiers	Fault ID	–
		Name	Yes
	Geographic characteristics	Country	Yes
		Physiographic province	Yes
		Exposure	–
	Seismic characteristics	Slip rates (geologic and geodetic)	Yes
		Historic earthquake	Yes
		Geomorphic expression	Yes
		Paleoseismic studies	Yes
	Structural characteristics	Primary sense of motion	Yes
		Strike and dip direction	–
		Length	–
	Description	Brief summary and remarks	–
	References	Citations	–

NHESSD
3, 5599–5632, 2015

Table 3. Description of parameters and fields used in the CAFD.

Database fields	Description
Name	The most commonly used fault name in the published literature. Name variations and spelling are included in the comment section.
Country	Name of countries where the fault trace is located.
Physiographical province	Name of regions with similar terrain and geologic history (e.g., Pamir, Tarim Basin, Alai Valley).
Exposure	Fault exposure level (exposed or concealed).
Geodetic slip rate ($mm\,yr^{-1}$)	The reported geodetic slip rate as documented in the original study. It is shown in $mm\,yr^{-1}$ and as a minimum-maximum range. Comments specific to the geodetic slip rate including all reported rates, types, uncertainties, references as well as methods are included in the comment section.
Geologic slip rate ($mm\,yr^{-1}$)	The reported Quaternary slip rate as documented in the original study. It is shown in $mm\,yr^{-1}$ and as a minimum-maximum range. Comments specific to the geologic slip rate including all reported rates, types, uncertainties, dating methods and references are included in the comment section.
Historic earthquake	Documented past earthquakes including location, magnitude, timing, related surface features (offsets, scarps, etc.), and references.
Geomorphic expression	Location and description of fault-related geomorphic markers (e.g., offset or deflected stream channels, sag ponds, scarps in young alluvium) as well as published analysis, interpretation and references.
Paleoseismic studies	Location and description of paleoseismic studies and references including trench site location and observations.
Primary sense of motion	The dominant style of faulting as reported in published literature. Comments specific to fault motion including changes in style of faulting along the strike as well as other documented components of movements and references are included in the comment section.
Dip direction	Dip direction of the main fault segment or fault zone. Comments specific to dip direction including reported direction for specific fault segments.
Strike	Strike of the main fault segment or fault zone. Comments specific to the strike of the fault including reported strikes for specific fault segments.
Length (km)	Length of the fault segment in kilometers. Comments specific to fault length including length of studied segments, total fault length and references are included in the comment section.
Description	A brief description of the fault and its geologic and tectonic settings.
References	References for fault parameters and trace(s) on the interactive map.

NHESSD
3, 5599–5632, 2015

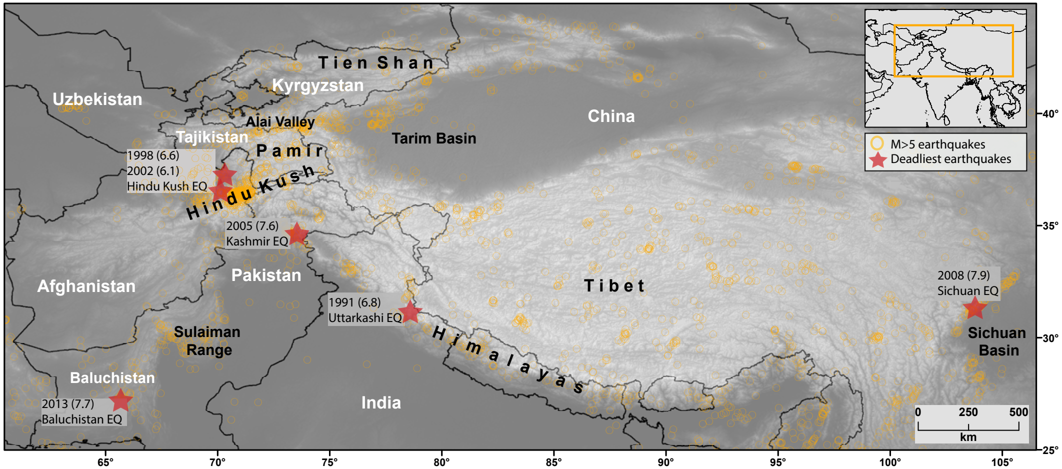

Figure 1. Map of the study area showing $M > 5$ earthquakes (orange circles) for the 1900–2014 period from ANSS Comcat (2014). Red stars mark the location of the deadliest earthquakes for the 1990–2014 period that are discussed in the text.

NHESSD
3, 5599–5632, 2015

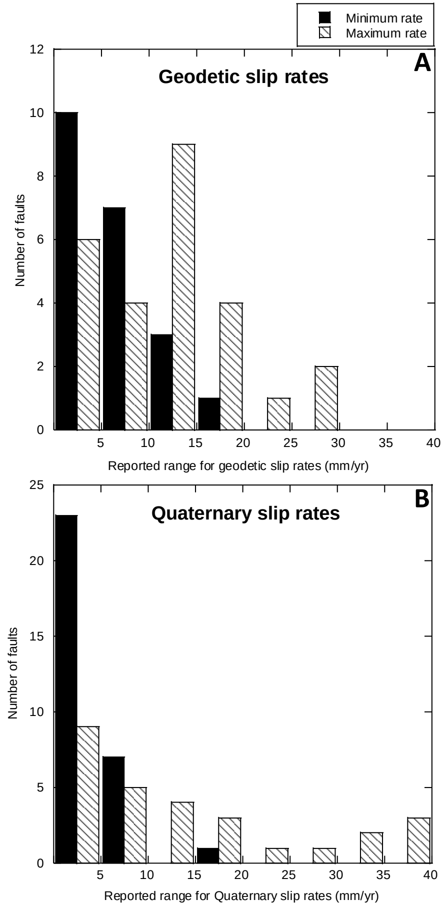

Figure 2. Distribution of geodetic **(a)** and geologic **(b)** slip rates as reported in the CAFD.

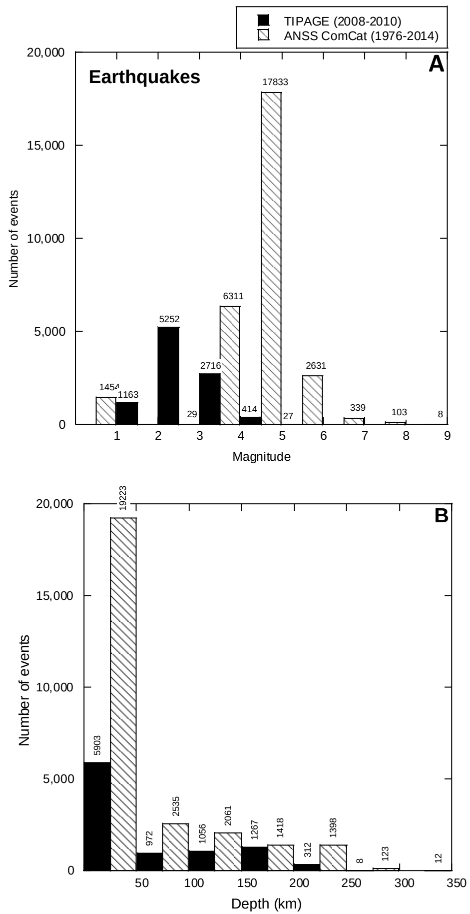

Figure 3. Earthquake distribution based on magnitudes **(a)** and depths **(b)** from global (ANSS ComCat) and regional (TIPAGE) catalogs.

NHESSD
3, 5599–5632, 2015

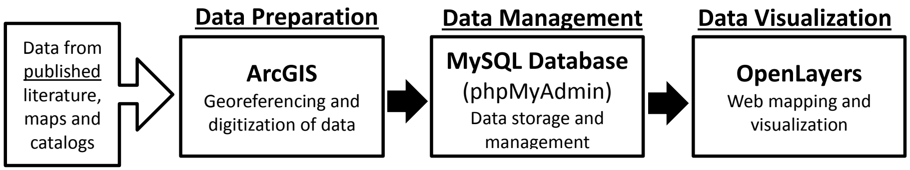

Figure 4. Flowchart of the process for the CAFD construction.

NHESSD
3, 5599–5632, 2015

A Quaternary Fault Database for Central Asia

S. Mohadjer et al.

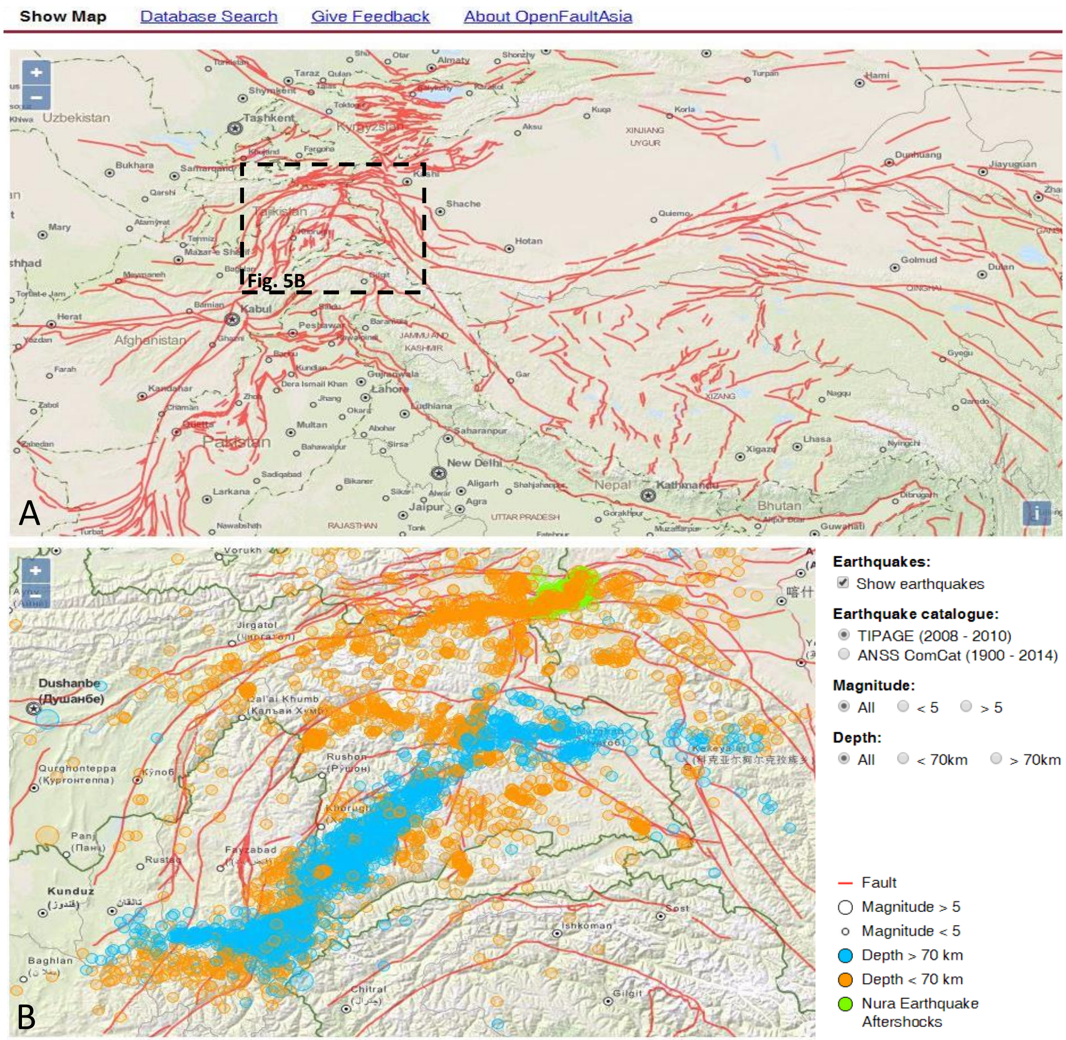

NHESSD
3, 5599–5632, 2015

A Quaternary Fault Database for Central Asia

S. Mohadjer et al.

Figure 5. The database interface includes an interactive fault map with faults shown in red **(a)**. Example of a map display with earthquake data set from Sipple et al. (2013) is shown for the Pamir and the Hindu Kush regions **(b)**. Black dashed box in **(a)** shows the map extent displayed in **(b)**.

NHESSD

3, 5599–5632, 2015

A Quaternary Fault Database for Central Asia

S. Mohadjer et al.

Show Map   Search Faults   Feedback   About

Chaman Fault

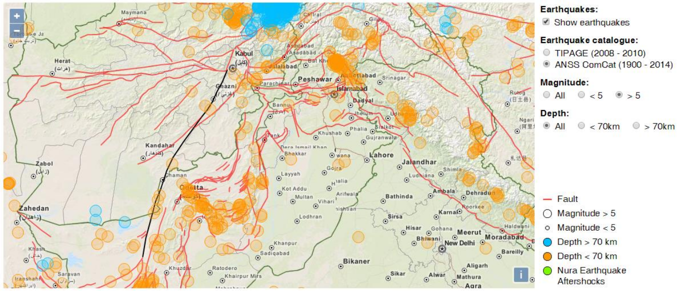

Name	Chaman Fault
comments	Also known as the Chaman Fault System. Ruleman et al. (2007) subdivided the system into four subsidiary systems including Chaman fault, Mokur fault, Gardiz fault, and Paghman fault

Geographic characteristics

Country	Afghanistan, Pakistan
Exposure	Exposed

Seismic characteristics

Geodetic slip rate (mm/yr)	5.4 - 16.8
comments	Based on geodetic observations, E. Apel (written commun., 2006, in Yeats, 2012) reported 26 mm/yr for the Chaman fault. This rate is close to that of 29.7 mm/yr predicted for relative movement of India toward Eurasia in this region (Sella et al., 2002). Mohadjer et al. (2010) used differences in velocities between GPS sites spanning most of the northern end of the Chaman Fault and placed a lower bound on the slip rate of 18 ± 1 mm/yr across this region. Furthermore, they estimated a rate of 5.4 ± 2 mm/yr of sinistral shear across the Gardiz and Mokur faults at the northern section of the Chaman Fault zone. Continental scale geodesy indicates that India's relative velocity with respect to Eurasia at the longitude of the Chaman fault system is 24-28 mm/yr of which 15.1 mm/yr is accommodated by the Ornach Nal fault and the central and southern Chaman fault (Szeliga et al., 2012). At latitude 33 degrees N and further north, InSAR data indicate a velocity across the Chaman fault of 16.8 ± 2.7 mm/yr near Qalat, Afghanistan (Szeliga et al., 2012). Based on GPS observations, the authors also reported 16.8 ± 0.51 mm/yr of sinistral motion near Kabul, Afghanistan.
InSAR	At latitude 33 degrees N and further north, InSAR data indicate a velocity across the Chaman fault of 16.8 ± 2.7 mm/yr near Qalat, Afghanistan (Szeliga et al., 2012). Based on GPS observations, the authors also reported 16.8 ± 0.51 mm/yr of sinistral motion near Kabul, Afghanistan.
Geologic slip rate (mm/yr)	2 - 40
comments	Based on the degree of topographic disturbance caused by the fault, Wellman (1965) suggested a present-day average slip rate of 2-20 mm/yr. Beun et al. (1979) suggested an average slip rate of 25-35 mm/yr over the last 2 My across the whole fault zone based on the correlation of Pliocene offset of volcanic units that straddle the fault north of Ab-e-Istada in Afghanistan. Geologic and plate closure estimates suggest sinistral slip across the Chaman fault system of between 19 and 35 mm/yr over the last 25 Ma (Lawrence and Yeats, 1979). NUVEL-1 global plate motion model of DeMets et al. (1990) predicts a rate of about 40 mm/yr for the Chaman Fault. Lawrence et al. (1992) reported 19-24 mm/yr over the last 20-25 My as a minimum slip rate assuming slip began just after the end of deposition of the Khojak Flysch. Yeats (2012) concluded that the slip rate on the Chaman Fault is high enough that the next earthquake is overdue, even assuming that some of the plate boundary slip maybe aseismic or on slow earthquakes. Although poorly constrained, Molnar et al. (2010) believe that the rate of slip on the Chaman Fault is >10 mm/yr and most likely between 20 and 30 mm/yr.
Historic earthquake	There are at least four major strike-slip earthquakes with M > 6 recorded historically on the Chaman fault: the 1505 earthquake (Ms 7.3) west of Kabul, the 1892 (Ms. 6.5) earthquake near the city of Chaman, the 1975 earthquake between Chaman and Nushki and the 1978 earthquake north of Nushki in Pakistan. No major historical earthquakes are noted between the 1892 Chaman rupture to the southern terminus of the 1505 rupture which made Bernard et al. (2000) and Ambraseys and Bilham (2003a) conclude that a significant slip deficit exists along the Chaman fault, especially north of ~31 degree latitude. The region east of the Chaman fault underwent two large earthquakes, the Mach earthquake of 27 August 1931 of Ms 7.3 in the Sibi re-entrant between the Brahui and Sulaiman ranges, and the Quetta earthquake of 30 May 1935 of Ms 7.7. The epicenter of the Quetta earthquake was close to the Ghazaband fault. Ambraseys and Bilham (1992), however, were unable to attribute the reported surface deformation to a source fault. Recent seismicity along the fault appears to be mostly small earthquakes (M 3-5), located mostly in regions with major historical seismicity. The M5 earthquake in 2005 ruptured the surface along the 6.5 km of the Chaman fault south of Kabul. The slow slip observed over a year after this event raises the possibility that other parts of the fault might rupture in slow slip events (Yeats, 2012).
Geomorphic expression	Earthquakes along the Chaman fault appear to consistently rupture to the surface. Oldham (1883) and Babur (1912) reported surface ruptures for the 1505 earthquake near Kabul. Griesbach (1893) observed surface rupture from the 1892 Chaman earthquake which offset railroad tracks crossing the fault by 0.75 m. No surface rupture has been reported for the 1975 Ms 6.7 earthquake which occurred between Nushki and Chaman in Pakistan. The 1978 Mw 6.1 earthquake near Nushki ruptured the surface (Yeats et al., 1979). Wellman (1965) reported stream offsets of 20-120 m. Active fault features consistent with the 1892 surface rupture are described by Lawrence and Yeats (1979).

Structural characteristics

Primary sense of motion	Sinistral (left-lateral); Strike-slip
comments	Ruleman et al. (2007) reported active frontal thrust faults along western margin of the Chaman fault. These arcuate, northwest-directed, east-dipping, frontal thrusts are second-order structures that result from the combination of compression and strike-slip motion on the Chaman fault system. Some of these thrust faults are >20 km long and extend >10 km west of the main fault trace. Multiple strike-slip fault strands are proximal to these thrust faults.
Length	> 850 km

References

Ambraseys and Bilham (2003b); Beun et al. (1979); DeMets et al. (1990); E. Apel (written commun., 2006); Griesbach (1893); Lawrence and Yeats (1979); Lawrence et al. (1992); Molnar et al. (2010); Sella et al. (2002); Szeliga et al. (2012); Wellman (1966); Yeats (2012)

NHESSD
3, 5599–5632, 2015

A Quaternary Fault Database for Central Asia

S. Mohadjer et al.

Figure 6. An example of a fault information page. The location map on top shows the selected fault in black (i.e., Chaman Fault). The fault description appears below the map. The description is organized into three distinct sections (i.e., geographic, seismic, and structural characteristics) with references linked to Google Scholar. Users can display earthquake data to visualize recorded seismicity in relation to the selected structure.

NHESSD
3, 5599–5632, 2015

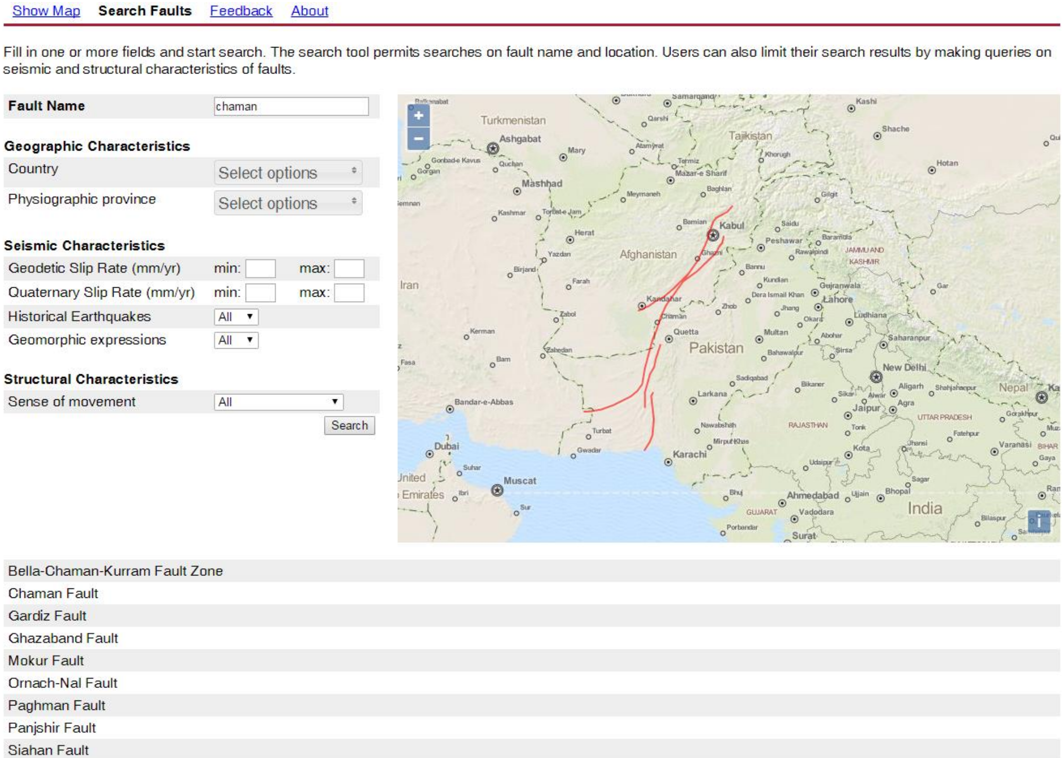

Figure 7. The database search tool allows users to search and sort fault information on a variety of fields. The above example shows search results for the Chaman Fault. The search yields results relevant to the Chaman fault including faults that are considered to be part of its extensions. These results are shown as a list and can be visualized on the map. Fault names and locations are linked to relevant fault information page.

NHESSD
3, 5599–5632, 2015

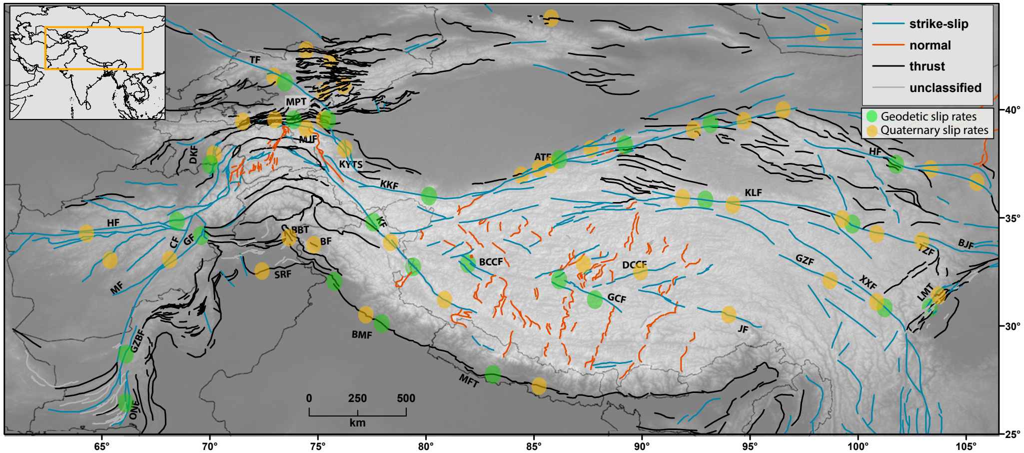

Figure 8. Locations of major active faults. Fault lines are color-coded based on their sense of movement. Locations of reported slip rates are marked with colored circles. Abbreviations of fault names: TF: Talas-Fergana fault; MPT: Pamir Main Thrust; MJF: Muji fault; DKF: Darvaz-Karakul fault; GF: Gardiz fault; CF: Chaman fault; MF: Mokur fault; GZBF: Ghazaband fault; ONF: Ornach-Nal fault; KF: Karakorum fault; KKF: Karakax fault; MFT: Main Frontal Thrust; BCCF: Bue Co Conjugate fault system; DCCF: Dong Co Conjugate fault system; JF: Jiali fault; GZF: Ganzi fault; XXF: Xianshuihe-Xiaojiang fault system; KLF: Kunlun fault; LMT: Longmen Shan thrust belt; TZF: Tazang fault; BJF: Bailong Jiang fault system; HF: Haiyuan fault; ATF: Altyn Tagh fault; SRF: Salt Range Front fault; BMF: Black Mango fault; BF: Balapora fault; GCF: Gyaring Co fault; HF: Herat fault; BBT: Balakot-Bagh Thrust; KYTS: Kashgar-Yecheng Transfer System.

NHESSD
3, 5599–5632, 2015